Earth and Planetary Science Letters 416 (2015) 35–45

Contents lists available at ScienceDirect

Earth and Planetary Science Letters

www.elsevier.com/locate/epsl

Geomagnetic paleointensity at ∼2.41 Ga as recorded by the Widgiemooltha Dike Swarm, Western Australia

Aleksey V. Smirnov [a,*], David A.D. Evans [b]

[a] Department of Geological and Mining Engineering and Sciences and Department of Physics, Michigan Technological University, Houghton, MI 49931, USA
[b] Department of Geology and Geophysics, Yale University, New Haven, CT 06520, USA

ARTICLE INFO

Article history:
Received 4 September 2014
Received in revised form 24 January 2015
Accepted 10 February 2015
Available online xxxx
Editor: J. Brodholt

Keywords:
paleointensity
Precambrian

ABSTRACT

Absolute geomagnetic paleointensity measurements were conducted on samples from six mafic dikes of the ∼2.41 Ga Widgiemooltha swarm (Western Australia). Rock magnetic analyses indicate that the paleointensity signal is carried by nearly stoichiometric pseudosingle-domain magnetite and/or low-Ti titanomagnetite. Paleointensity values were determined using the Thellier double-heating method supplemented by low-temperature demagnetizations (the LTD-Thellier method) in order to reduce the effect of magnetic remanence carried by large pseudosingle-domain and multidomain magnetite grains. Thirty-one samples from five dikes yielded successful paleointensity determinations with the mean value of 41.2 ± 3.8 μT, which corresponds to a virtual dipole moment of 6.65 ± 0.98 A m^2. The mean and range of paleofield strength values are similar to those of the recent Earth's magnetic field and are consistent with a compositionally driven geodynamo established by the earliest Paleoproterozoic Era. The existence of a stable, dipolar geomagnetic field during the Proterozoic indicated by paleointensity and paleodirectional data from this and prior studies seems incompatible with a young age of the inner core suggested by recent models of the Earth's thermal evolution. Acquisition of reliable paleointensity estimates using the novel approaches such as the LTD-Thellier method is crucial in constraining the development of more realistic, Earth-like models of long-term geodynamo behavior.

1. Introduction

Data on the long-term behavior and configuration of the geomagnetic field during the Precambrian are crucial for understanding the nature of Earth's early geodynamo and constraining models of planetary evolution (e.g., Coe and Glatzmaier, 2006; Evans, 2006; Aubert et al., 2010; Smirnov et al., 2011). These data are also indispensable for deciphering potential causative links between the evolution of geomagnetic field and other components of the Earth system. For example, a weak or unstable field of an early geodynamo could result in a stronger effect on the atmosphere and biosphere from solar and cosmic radiation (e.g., Sinnhuber et al., 2003; Ozima et al., 2008; Tarduno et al., 2010, 2014). However, our knowledge of the Precambrian geomagnetic field remains very limited, especially with regard to the field strength (paleointensity), which represents one of the most challenging aspects of paleomagnetic research (e.g., Tauxe and Yamazaki, 2007).

The Precambrian paleointensity database comprises less than five per cent of the total paleointensity database and is characterized by an uneven temporal and spatial distribution (e.g., Smirnov et al., 2003; Tauxe and Yamazaki, 2007; Biggin et al., 2009). Moreover, many of the Precambrian paleointensity results are based on a small number of cooling units (e.g., Morimoto et al., 1997), and some data clearly reflect alteration processes (e.g., Yoshihara and Hamano, 2004). Consequently, the database does not yet provide a reliable picture of the long-term changes of the Earth's magnetic field strength in the Precambrian.

The majority of paleointensity determinations for the Phanerozoic are derived from extrusive rocks (mostly basaltic lavas) using variations of the Thellier double-heating method (Thellier and Thellier, 1959). However, many Precambrian extrusive sequences have been lost to erosion, and the remaining rocks are often affected by weathering, deformation, and/or metamorphism, hindering the preservation and measurement of paleointensity signal using the Thellier approach. Because of the rarity of well-preserved extrusive Precambrian rocks, relatively quickly cooled shallow intrusions such as mafic dikes and sills represent an attractive alternative target for paleointensity studies. Prominent globally distributed mafic dike swarms represent the feeder systems of large igneous provinces (e.g., Ernst and Buchan, 1997) and often preserve pristine paleomagnetic and geochemical signatures

* Corresponding author.
E-mail address: asmirnov@mtu.edu (A.V. Smirnov).

http://dx.doi.org/10.1016/j.epsl.2015.02.012
0012-821X/

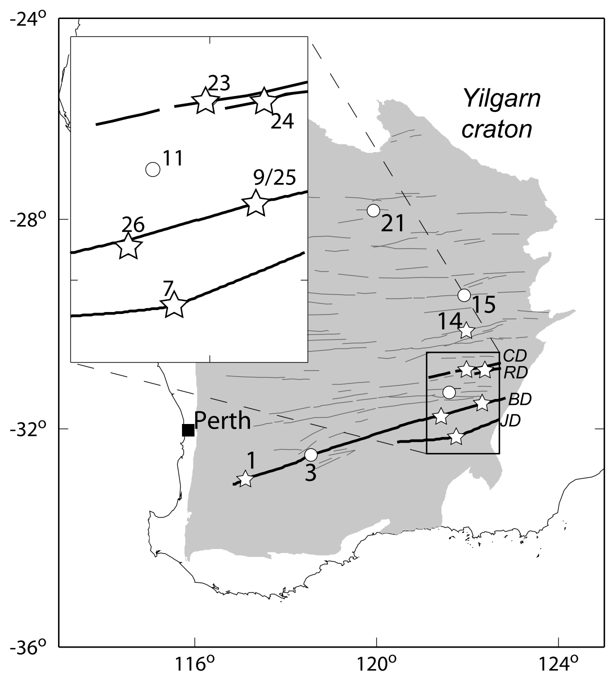

Fig. 1. Locations of sampling sites used for rock-magnetic and paleointensity analyses in this study. The site numbers correspond to the numeration used in Smirnov et al. (2013). Stars indicate the sites that yielded three or more successful paleointensity determinations (Table 1). Thin lines within the Yilgarn craton (shaded area) indicate the Widgiemooltha dike swarm; thicker solid lines show the Binneringie (BD), Jimberlana (JD), Celebration (CD) and Randalls (RD) Dykes.

(e.g., Halls, 2008). Several dike swarms have been successfully used for paleointensity determinations (e.g., Macouin et al., 2003, 2006; Smirnov et al., 2003; Halls et al., 2004; Shcherbakova et al., 2008).

The Thellier method is ultimately based on the laws of reciprocity, independence, and additivity for partial thermal remanent magnetization (pTRM) (Thellier, 1941). The Thellier laws hold to a good approximation if the magnetization is carried by single-domain (SD) or smaller pseudosingle-domain (PSD) magnetic grains, but are violated for larger PSD and multidomain (MD) carriers (e.g., Shashkanov and Metallova, 1972; Bolshakov and Shcherbakova, 1979; Shcherbakov and Shcherbakova, 2001). The presence of such "non-ideal" grains in many rocks renders paleointensity determination difficult or sometimes impossible (e.g., Xu and Dunlop, 2004).

In order to extend the applicability of the Thellier method to rocks containing larger PSD and MD magnetite grains, integration of the Thellier technique with low-temperature demagnetization (LTD) was suggested (e.g., Schmidt, 1993). Low-temperature demagnetization consists in temperature cycling of a magnetite-bearing sample through the crystallographic Verwey transition of magnetite at ~120 K (Verwey, 1939) in a magnetic field-free environment. LTD selectively removes or minimizes the signal carried by non-ideal MD and large PSD grains (e.g., Ozima et al., 1964; Levi and Merrill, 1978). Some studies suggest (e.g., Kosterov et al., 2009; Engelmann et al., 2010) that LTD may also have a similar effect for low-Ti titanomagnetites (up to 55% Ti content) due to the presence of an isotropic point (Syono, 1965; Kakol et al., 1991). Thellier experiments combined with LTD (the LTD-Thellier method) have resulted in a higher success rate and better quality of paleointensity results from extrusive and intrusive rocks (Schmidt, 1993; Celino et al., 2007; Kulakov et al., 2013).

In this paper, we report new absolute paleointensity data obtained using the LTD-Thellier method from the ~2.41 Ga Widgiemooltha mafic Dike Swarm in Western Australia, and discuss the implications of our results for the early geodynamo.

2. Widgiemooltha Dike Swarm

The generally east–west trending dikes of the Widgiemooltha swarm outcrop over the entire Yilgarn craton in Western Australia (e.g., Sofoulis, 1966; Parker et al., 1987) (Fig. 1). Most of the dikes have picrite, olivine–dolerite or quartz–dolerite composition and have not been affected by significant metamorphic events since their formation (e.g., Hallberg, 1987). A baddeleyite U–Pb age of 2418 ± 3 Ma was reported for the westernmost extension of the ~600-km-long Binneringie Dyke (Nemchin and Pidgeon, 1998), while a slightly younger age of 2410.3 ± 2.1 Ma was obtained by electron microprobe U–Pb analyses of baddeleyites from an eastern location in the same dike (French et al., 2002). Doehler and Heaman (1998) reported a baddeleyite U–Pb age of $2410.6 + 2.1/-1.6$ Ma for the Celebration Dyke. Finally, an Rb–Sr and Sm–Nd isochron age of 2411 ± 38 Ma was reported for the ultramafic core of the ~180-km-long Jimberlana intrusion (Fletcher et al., 1987). The consistency of isotopic ages further indicates the excellent preservation of the dikes.

Well-defined characteristic remanent magnetization (ChRM) directions with the mean of $D = 247.5°$, $I = -66.6°$ ($\alpha_{95} = 4.8°$) were obtained from thirteen sites representing nine separate dikes (Smirnov et al., 2013; incorporating data from Evans, 1968). The primary origin of ChRM has been confirmed by baked-contact tests. The corresponding paleomagnetic pole, located at 10.2°S, 159.2°E ($A_{95} = 7.5°$, $N = 9$ dikes) (Smirnov et al., 2013), has the highest score ($Q = 7$) on the paleomagnetic reliability scale (Van der Voo, 1990).

For this study, we conducted rock magnetic and paleointensity analyses on samples from eleven sites representing eight of the nine dikes that yielded the Widgiemooltha ChRM directions (Smirnov et al., 2013). Unfortunately, no material from the single measured reversely-magnetized Widgiemooltha dike (Site H from Evans, 1968) was available for this study.

3. Magnetic mineralogy

We conducted rock magnetic and scanning electron microscope analyses of the selected Widgiemooltha dikes in order to determine their magnetic mineralogy and suitability for paleointensity experiments. The opaque mineralogy of our samples was examined using a model JEOL JSM-6400 scanning electron microscope (SEM) equipped with an energy dispersive spectra (EDS) detector. Backscattered electron imaging was used to identify oxide grains. The grains varied in size from over a hundred microns to less than five microns, containing one or several subordinate sets of lamellae at micron to sub-micron scale (Fig. 2a–f).

The composition of the oxide grains was determined by means of energy dispersive spectrometry. The EDS analyses showed that the bright areas in the oxide grains separated by lamellae represent an iron oxide phase with no or very low titanium content (Fig. 2g). The spectra measured from the darker phase (lamellae) indicate an iron–titanium oxide with a higher Ti content (Fig. 2h). Similar exsolution lamellae were observed for the Jimberlana Dyke by McClay (1974). We note that exact measurement of the iron and titanium content was not possible because of the relatively large interaction volume of the electron beam (~2 μm). No homogeneous iron–titanium oxide, iron oxide, or titanium oxide grains were identified by the SEM analyses. In some samples, rare grains of chalcopyrite and pyrite were found.

Temperature dependences of low-field magnetic susceptibility, $\kappa(T)$, were measured upon cycling from room temperature to 700 °C (in argon) using an AGICO MFK1-FA magnetic susceptibility meter equipped with a high-temperature furnace and a cryostat. The $\kappa(T)$ curves were also measured during heating from −192°C

Table 1
Summary of paleointensity data from the Widgiemooltha dikes. n and s: the number of samples and specimens measured; N: the number of samples with accepted paleointensity determination; H: site-mean paleofield intensity and its standard deviation (dH); λ_{paleo}: paleolatitude used to calculate site-mean virtual dipole moment (VDM) with its standard deviation ($dVDM$); f and q: the fraction of the NRM and the quality factor (Coe et al., 1978) with their standard deviations ($S.D.$).

Site	$n/s/N$	H (μT)	dH (μT)	λ_{paleo} (°)	VDM ($\times 10^{22}$ A m^2)	$dVDM$ ($\times 10^{22}$ A m^2)	$f \pm S.D.$	$q \pm S.D.$
Site 1[a]	7/13/5	40.3	1.4	45.3	6.80	0.23	0.82 ± 0.05	14.0 ± 6.8
Site 26[a]	6/10/5	44.3	1.5	49.1	6.95	0.24	0.88 ± 0.02	15.0 ± 4.4
Site 9, 25[a]	8/16/4	46.0	3.1	49.9	7.17	0.39	0.84 ± 0.06	13.7 ± 7.1
Binneringie Dyke mean	*3*	*43.5*	*2.9*	–	*6.97*	*0.19*	–	–
Site 7[b]	7/14/4	42.4	1.7	50.8	6.55	0.26	0.85 ± 0.02	18.5 ± 9.3
Site 14	8/13/6	45.4	1.9	36.9	8.13	0.33	0.86 ± 0.03	14.7 ± 9.6
Site 15[*]	4/8/2	43.6	3.1	52.2	6.65	0.48	0.83 ± 0.02	13.1 ± 1.7
Site 23[c]	4/8/3	39.0	2.0	51.2	6.01	0.30	0.83 ± 0.06	16.8 ± 7.5
Site 24[d]	6/10/4	35.8	2.3	50.0	5.57	0.35	0.87 ± 0.05	14.9 ± 8.2
Total mean	*46/84/31*	*41.2*	*3.8*	–	*6.65*	*0.98*	–	–

[a] Binneringie Dyke; [b] Jimberlana Dyke; [c] Celebration Dyke; [d] Randalls Dyke (sites 14 and 15 represent the dikes that have not been individually named in the official nomenclature); [*] Site 15 data were not used in the total mean calculation.

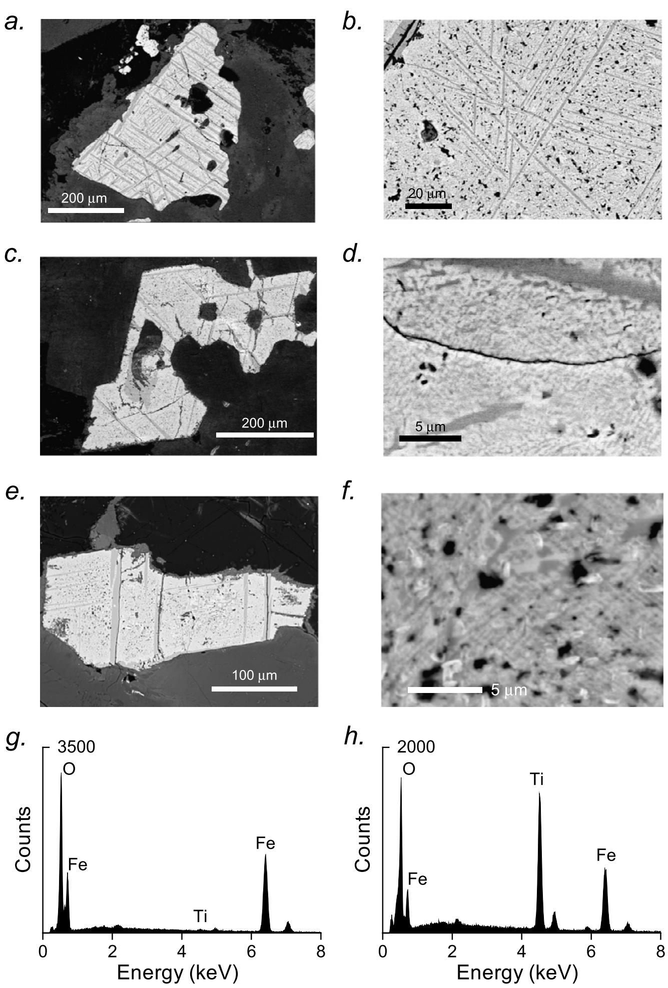

Fig. 2. **(a, c, e)** Examples of backscattered electron images of magnetic grains of the Widgiemooltha dikes showing intergrowths of no/low-Ti (lighter areas) and high-Ti (darker areas) phases. **(b, d, f)** Examples of finer intergrowth of the no/low- and high-Ti phases within grain interiors (see text). **(g, h)** Typical energy dispersive spectra from the **(g)** no/low-Ti and **(h)** high-Ti phases, interpreted as magnetite and ilmenite/ulvospinel, respectively (see text).

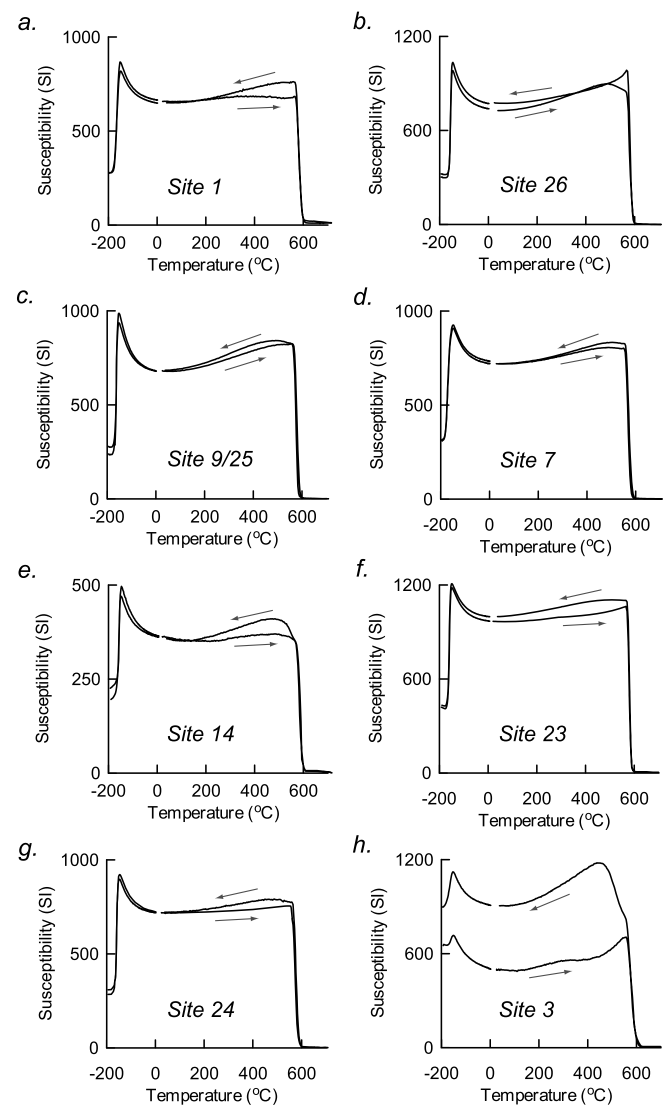

Fig. 3. **(a–g)** Examples of dependences of low-field magnetic susceptibility (κ) versus temperature for the Widgiemooltha sites that yielded successful paleointensity determinations (Table 1). **(h)** An example of irreversible $\kappa(T)$ curve for a sample rejected from paleointensity experiments (see text). Arrows show the direction of temperature change. The peak at about −153 °C corresponds to the Verwey transition of magnetite (Verwey, 1939). Sites 1, 3, 26, 9/25 represent the Binneringie Dyke; Site 7, the Jimberlana Dyke; Site 14, an unnamed dike; Site 23, the Celebration Dyke; Site 24, the Randalls Dyke (Fig. 1).

to room temperature both before and after the high-temperature thermomagnetic runs (Fig. 3).

For eight sites, many samples yielded (nearly)-reversible $\kappa(T)$ curves revealing the presence of a magnetic phase with Curie temperatures in a range of 560 °C to 585 °C, indicating magnetite to low-Ti titanomagnetite as a magnetic carrier (Fig. 3a–g). When heated in argon, most samples show a gradual increase of κ, followed by a sharp decrease of κ to the Curie temperature (Fig. 3a–g). Such a behavior is characteristic for pseudosingle-domain (PSD) magnetite grains (e.g., Dunlop, 1974; Clark and Schmidt, 1982). No or negligible change of room-temperature magnetic susceptibility suggests the absence of significant alteration in these samples. The difference between the heating and cooling legs of $\kappa(T)$ curves observed at high temperatures likely reflects a non-unique response of PSD and MD grains to the applied magnetic field due to relaxation of internal stress by heating (e.g., Kosterov and Prévot, 1998). The presence of a characteristic peak at about −153°C, associated with the Verwey transition further indicates the presence of nearly-stoichiometric magnetite.

For three sites, all measured samples yielded irreversible $\kappa(T)$ curves, typically indicating formation of additional magnetic material (Fig. 3h). In many such samples, the post-heating low-temperature run was characterized by a more expressed Verwey transition peak, suggesting that the new magnetic phase is magnetite. The new magnetite may be a product of heating-induced transformation of clays (e.g., Hirt and Gehring, 1991) or form by continued exsolution of titanomagnetite grains into a high-Ti and magnetite (low-Ti) phases (e.g., Smirnov et al., 2005). Regardless of the alteration mechanism, the samples manifesting the irreversible $\kappa(T)$ curves were not used for paleointensity experiments.

Magnetic hysteresis parameters (coercivity, H_c; coercivity of remanence, H_{cr}; saturation remanence, M_r; and saturation magnetization, M_s) were measured using a Model 2900 Princeton Measurement Corporation Alternating Gradient Field Magnetometer. The hysteresis measurements indicate a pseudosingle domain (PSD) magnetic carrier in all samples (Fig. 4), consistent with the results of our thermomagnetic analyses and with the characteristic size (sub-micron to microns) of the magnetite regions intergrown with a high-Ti phase observed by SEM. For several samples that yielded nearly-reversible $\kappa(T)$ curves, magnetic hysteresis was also measured after temperature cycling of the samples to 600 °C. Most of the samples showed no or negligible change in hysteresis behavior after the temperature treatment, further confirming their magnetic stability with respect to the laboratory heating.

4. Paleointensity determination

4.1. Experimental technique

The paleointensity analyses were performed on cylindrical mini-specimens (10 mm diameter, 10 mm length) (e.g., Leonhardt et al., 2000; Celino et al., 2007; Muxworthy et al., 2013) representing 50 samples using the Thellier double-heating method modified by Coe (1967) and Coe et al. (1978) (Table 1). Magnetic remanence of the specimens was measured using a 2 G DC superconducting quantum interference device (SQUID) magnetometer housed in magnetically shielded environment. The specimens were heated in an ASC TD-48SC thermal specimen demagnetizer with controlled atmosphere (nitrogen) chamber. The specimens were always placed in the furnace at exactly the same location and with the same orientation relative to the applied magnetic field. A laboratory field of 50 μT was used for in-field steps to impart partial thermal remanent magnetizations (pTRMs).

After measurement of NRM from each sample, the first heating in our experiments was done to 400 °C to eliminate the low-temperature component of NRM in a single step and reduce the chance of heating-induced alteration. Temperature increments were adjusted to best record the component with high unblocking temperatures (400 °C; 450 °C; 475 °C, 510 °C, 10 °C step in 525–585 °C range, 600 °C).

In order to reduce the effect of magnetic remanence carried by large PSD and MD grains, samples were subjected to three low-temperature demagnetizations (LTD) in liquid nitrogen after the measurement of NRM and after each heating (e.g., Kobayashi and Fuller, 1968; Celino et al., 2007; Kulakov et al., 2013). The magnetic remanence was measured after LTD treatment and, for the Binneringie Dyke samples, also before LTD. After the experiment, the measured data were plotted on an Arai (NRM-remaining versus pTRM-gained) plot (Arai, 1963; Nagata et al., 1963) (Figs. 5 and 6). The paleointensity data processing was done using the ThellierTool-4.22 program (Leonhardt et al., 2004).

To monitor possible alteration during the paleointensity experiment, pTRM checks (Coe et al., 1978) were utilized for temperature steps above 510 °C: after every second off-field temperature step, an on-field step at a lower temperature was measured. An additional pTRM check for 575 °C was done after heating to 600 °C. A pTRM check was accepted if it fell within 10% of the original pTRM value. In addition, we used the following reliability criteria: (1) The linear segment on the Arai plot used to calculate the paleofield is based on at least 5 data points and represents at least 50% of natural remanent magnetization (fraction of NRM, f, as defined by Coe et al., 1978); (2) The quality factor q (Coe et al., 1978) is five or greater; (3) The directional data of the zero-field steps must have a maximum angle of deviation (MAD) less than 10°. A mean paleointensity value for a site was accepted if it was based on successful determinations from at least three samples.

Overall, paleointensity determinations from 33 samples (eight sites) representing six dikes were accepted based on our reliability criteria (Table 1). Twenty-eight accepted determinations belonged to Class A and five to Class B as defined by the criteria incorporated in the ThellierTool-4.22 program (Leonhardt et al., 2004). Most rejected determinations had the quality factor less than five, or failed the pTRM checks. No obvious correlation was observed between the rock magnetic properties and success of paleointensity determination from a sample (Fig. 4e).

4.2. Paleointensity results

For all measured samples, demagnetization of NRM by zero-field temperature steps yielded a stable characteristic remanent magnetization component identified by straight linear demagnetization trajectory towards to the origin of vector end-point diagrams (Figs. 5 and 6). The ChRM directions were statistically similar to the directions obtained from the corresponding samples in our companion paleomagnetic directional study of the Widgiemooltha dikes (Smirnov et al., 2013).

All accepted samples manifested linear behavior on the LTD-Thellier Arai plots above 510–525 °C (Figs. 5 and 6). While the initial LTD resulted in removal of a part of the original NRM, subsequent LTDs during the paleointensity experiments resulted almost entirely in partial demagnetization of the pTRM-gained while the NRM remaining after each temperature step was not significantly affected (Fig. 5). For our paleointensity determinations, we used a high-temperature part of the Arai plot above 510–525 °C (Table 1).

Three sites (14 samples) representing the Binneringie Dyke (Sites 1, 9/25, and 26) yielded consistent paleointensity values with the mean of 43.5 ± 2.9 μT (the mean virtual dipole moment, VDM, is $6.97 \pm 0.19 \times 10^{22}$ A m^2) (Table 1). Four samples from Site 7 (the Jimberalana Dyke) yielded the mean paleointensity of 42.4 ± 1.7 μT (VDM = $6.55 \pm 0.26 \times 10^{22}$ A m^2). Six successful paleointensity determinations with the mean of 45.4 ± 1.9 μT (VDM = $8.13 \pm 0.33 \times 10^{22}$ A m^2) were obtained from Site 14. Three and four paleointensity determinations were accepted for Sites 23 (the Celebration Dyke) and 24 (the Randalls Dyke), respectively, with the corresponding mean values 39.0 ± 1.8 μT (VDM =

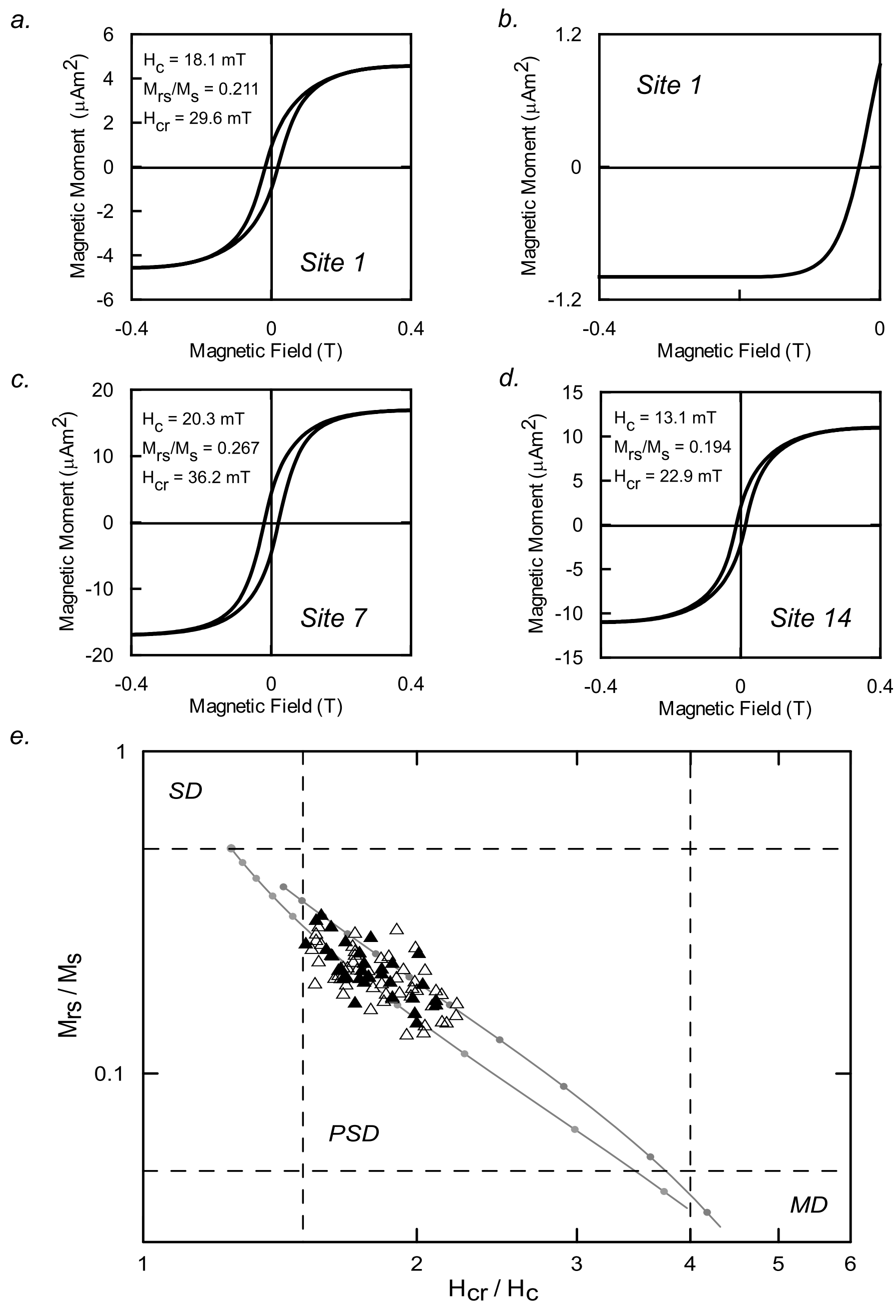

Fig. 4. **(a, c, d)** Typical magnetic hysteresis loops (after paramagnetic slope correction) for the Widgiemooltha dike sites that yielded successful paleointensity determinations. **(b)** An example of backfield demagnetization of saturation remanence. **(e)** The Day plot (Day et al., 1977). Solid/open triangles show the data from samples that resulted in successful/failed paleointensity determinations. Abbreviations are: H_c, coercivity; H_{cr}, coercivity of remanence; M_{rs}, saturation remanence; M_s, saturation magnetization; SD, single-domain; PSD, pseudosingle-domain; MD, multidomain; SP, superparamagnetic. Also shown are SD-MD mixture models from Dunlop (2002). Site 1 represents the Binneringie Dyke; Site 7, the Jimberlana Dyke; Site 14, an unnamed dike (Fig. 1).

$6.01 \pm 0.27 \times 10^{22}$ A m^2) for Site 23 and 35.8 ± 2.3μT (VDM = $5.57 \pm 0.35 \times 10^{22}$ A m^2) for Site 24. The grand mean paleointensity calculated from all five dikes is 41.2 ± 3.8 μT, and the mean VDM is 6.65 ± 0.98 A m^2 (Table 1; Fig. 7).

A difference in cooling rate between the natural remanence and laboratory pTRM acquisitions may result in an overestimation (e.g., Dodson and McClelland-Brown, 1980; Halgedahl et al., 1980) or underestimation (McClelland-Brown, 1984) of paleointensity for rocks containing SD or MD magnetic carriers, respectively. We used a conductive cooling model (Jaeger, 1968) to calculate the time required for two sites (Site 1 and Site 9/25) representing the Binneringie Dyke (the largest Widgiemooltha dike) to cool from 580 °C to 510 °C (approximately the maximum and minimum laboratory unblocking temperatures of our samples). Assuming that 1200 °C magma intruded a 20 °C country rock in a single event, the time was found to be ∼ 150 years for Site 1 (∼350 m width) and ∼ 950 years for Site 9/25 (∼1000 m width).

Intrusion into a deeper-seated, and thus hotter, country rock would reduce the cooling rate. For example, for intrusion into a 200 °C country rock, the calculated cooling times for Sites 1 and 9/25 are ∼450 and 1900 years, respectively. If our rocks contained ideal SD magnetic grains and the dikes were intruded into hot crust, the corresponding Thellier data could overestimate the true field by ∼34–37% for these sites (Halgedahl et al., 1980). However, our SEM analyses indicate that the Widgiemooltha samples do not contain true SD grains. Instead, the "post-LTD" remanences,

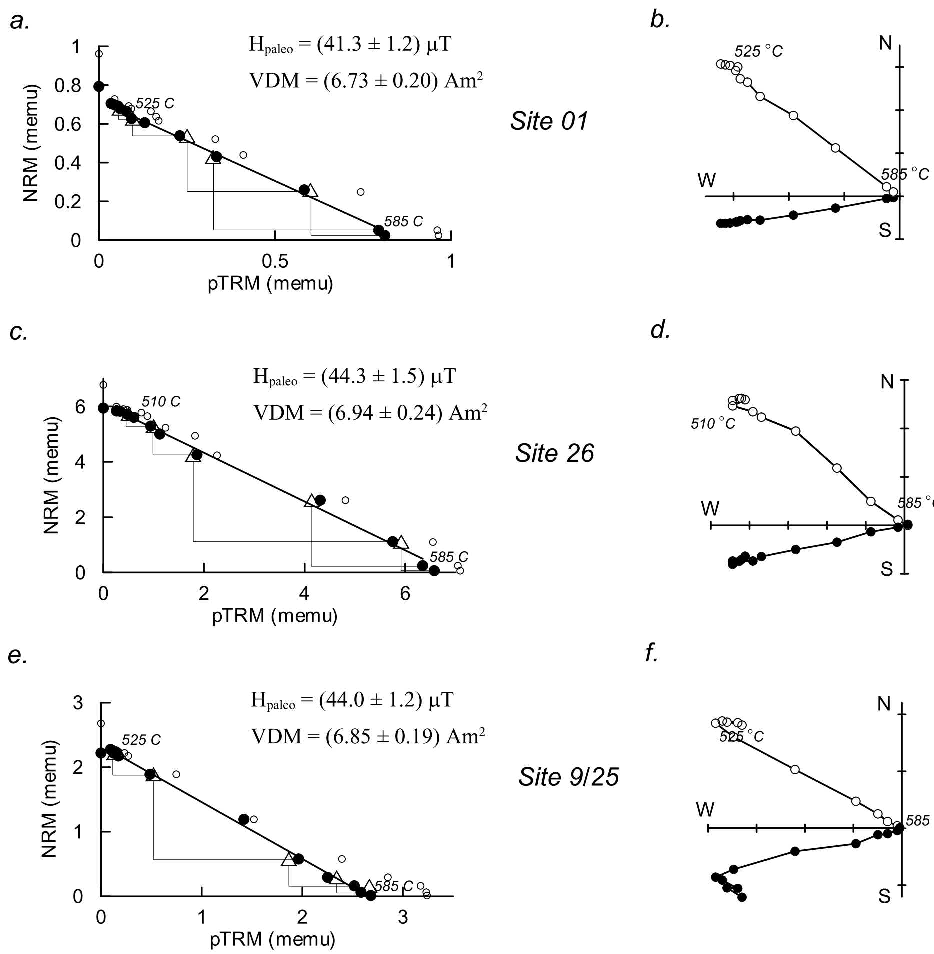

Fig. 5. Examples of successful LTD-Thellier paleointensity determinations from the Binneringie Dyke (Sites 1, 25, and 26). **(a, c, e)** Natural remanent magnetization lost partial thermoremanent magnetization gained (solid circles). Open circles show the data measured before low temperature demagnetization (see text). Temperatures shown on the Arai plots specify the temperature range to find the best fit line. Triangles are partial TRM checks. **(b, d, f)** Orthogonal vector plots of field-off steps (vertical projection of NRM, open circles; horizontal projection of NRM, closed circles).

resulting in the linear SD-like Arai plots, are likely to be carried by small PSD grains and/or "magnetically-hard" domain structures within larger PSD grains (e.g., Dunlop and Özdemir, 1997). We note that recent theoretical and experimental results (Winklhofer et al., 1997; Yu, 2011; Ferk et al., 2014) suggest that the cooling rate correction for PSD grains is negligible. In addition, the Binneringie Dyke calculations above represent the maximum possible cooling times in this study, as those sites are from the greatest widths of the intrusions; consistency of VDM values from Widgiemooltha dikes of varying widths supports the notion that variable cooling rates did not bias the paleointensity results. Accordingly, we did not apply cooling rate corrections to our paleointensity results.

5. Discussion

5.1. Paleointensity determinations from the Widgiemooltha dikes

Our rock magnetic analyses show that some of the Widgiemooltha dikes possess rock magnetic characteristics which make them suitable for paleointensity experiments using the LTD-Thellier method and are likely to retain a pristine record of the strength of Earth's magnetic field that existed at ~2.41 Ga. The incorporation of low-temperature demagnetization into the Thellier protocol has resulted in linear high-temperature segments on Arai plots and relatively high quality factors of paleointensity determinations (Table 1). The experimental success rate of ~37 per cent is comparable with that of the paleointensity studies of much younger rocks. Overall, we feel that the LTD-Thellier values provide accurate estimates of the paleofield intensity because the LTD removes the adverse effects associated with magnetizations of PSD and MD magnetite grains.

The angular dispersion of virtual geomagnetic poles $S = (12.2 \pm 4.0)^\circ$ calculated for the five dikes that yielded accepted paleointensity determinations is indistinguishable from the value of $S = (11.7 \pm 1.9)^\circ$ calculated for the entire paleodirectional Widgiemooltha dataset (Smirnov et al., 2013). Although this similarity can be fortuitous because of the limited number of independent cooling units (5 dikes), it indicates that our mean paleointensity value may represent a time-averaged field reasonably well.

Although nearly stoichiometric magnetite is the dominant carrier of paleointensity signal in our samples as indicated by thermomagnetic analyses (Fig. 3), the samples may contain a small amount of magnetic grains that are unaffected by LTD. For example, greater than 3% Ti substitution for Fe in magnetite completely suppresses the Verwey transition (e.g., Kakol et al., 1992) and greater than ~15% Ti content in titanomagnetite shifts the isotropic temperature below 77 K (e.g., Kakol et al., 1991). The presence of such grains would result in a shallowing of the Arai linear segment used for paleointensity calculation. Hence, we cannot rule out that some of our values slightly underestimate the field strength.

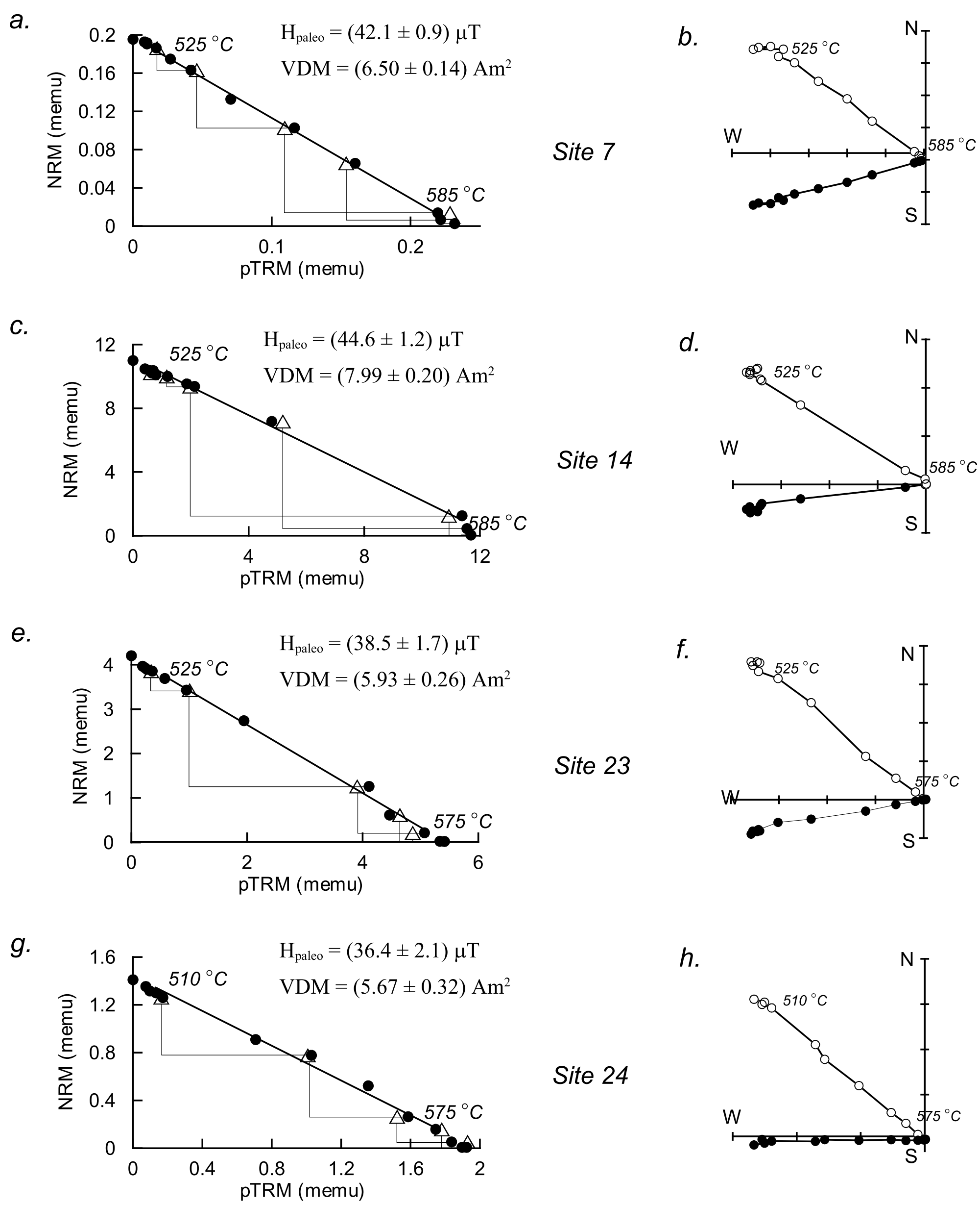

Fig. 6. Examples of LTD-Thellier paleointensity determinations from Sites 7 (the Jimberlana Dyke), 14 (an unnamed dike), 23 (the Celebration Dyke), and 24 (the Randalls Dyke). **(a, c, e, g)** Natural remanent magnetization lost partial thermoremanent magnetization gained (solid circles). Temperatures shown on the Arai plots specify the temperature range to find the best fit line. Triangles are partial TRM checks. **(b, d, f, h)** Orthogonal vector plots of field-off steps (vertical projection of NRM, open circles; horizontal projection of NRM, closed circles).

The presence of low- and high-Ti phase intergrowths in the Widgiemooltha dikes (Fig. 2) also suggests a possibility that their characteristic remanence may include a thermochemical remanent magnetization (TCRM) (e.g., Smirnov and Tarduno, 2005). A TCRM is imparted if the (oxy)exsolution process during initial lava cooling continues at temperatures below the Curie point of magnetite (Nagata and Kobayashi, 1963). Smirnov and Tarduno (2005) suggested that the presence of TCRM in intrusive rocks may lead to an underestimate of the true field value without violating experimental selection criteria of the Thellier method. Although the effect of TCRM on paleointensity determinations is still poorly understood and is difficult to estimate quantitatively (e.g., Fabian, 2009), we cannot completely exclude the possibility of a low-field bias in some of our paleointensity estimates due to the presence of a TCRM. We note that the incorporation of LTD to the Thellier protocol would not correct for such a TCRM-related bias.

5.2. Comparison with the early Paleoproterozoic–Neoarchean paleointensity data

The Precambrian paleointensity database is very sparse, with data points commonly separated by tens or even hundreds of millions of years. The current database can thus only reflect very-long term data trends such as a hypothetical sharp increase in the field strength associated with the start of modern compositional geodynamo (e.g., Stevenson et al., 1983), or a variation of paleointensity related to long-term changes in the mantle convection affecting the forcing of the geodynamo (e.g., Tarduno et al., 2006). Below, we compare our Widgiemooltha results with the other paleointensity data for the early Paleoproterozoic and Neoarchean Eras (2100–2900 Ma) (Table 2; Fig. 7).

The paleointensity data closest in time to our Widgiemooltha dike study are from the border dikes of the ~2.45 Ga Burakovka layered intrusion (Karelia, Russia). Fifteen successful Thellier anal-

Table 2
Paleointensity results for the Neoarchean and early Paleoproterozoic (2000–2900 Ma) based on the Thellier (TC) and microwave (MW) methods. VDM is the mean VDM with 1σ uncertainty, B/N is the number of sites/samples used to calculate the mean VDM.

Rock unit	Letter code	Age (Ma)	VDM ($\times 10^{22}$ A m^2)	B/N	Method	Reference
Fort Frances dikes (Canada)	FM	2076 ± 5	1.07 ± 0.16	3/7	TC	Macouin et al. (2003)
	FH		3.88 ± 0.63	3/3	MW	Halls et al. (2004)
Marathon dikes (Canada), R-polarity	MR	2104 ± 5	1.72 ± 0.14	2/2	MW	Halls et al. (2004)
Marathon dikes (Canada), N-polarity	MM	2121 ± 14/7	1.03 ± 0.22	4/12	TC	Macouin et al. (2003)
	MH		3.68 ± 0.98	3/4	MW	Halls et al. (2004)
Biscotasing dikes (Canada)	BM	2167 ± 2	0.85 ± 0.10	2/6	TC	Macouin et al. (2003)
	BH		5.85 ± 1.69	4/4	MW	Halls et al. (2004)
Senneterre dikes (Canada)	ST	2216 ± 8/4	1.26 ± 0.87	1/4	TC	Macouin et al. (2003)
Dharwar dikes (India)	DW	2367± 2	1.3± 1.0	2/24	TC	Valet et al. (2014)
Widgiemooltha dikes (Western Australia)	W	2414 ± 3	6.65 ± 0.98	8/31	TC	This study
Burakovka border dikes (Russia)	BR	2449 ± 1	8.43 ± 2.11	4/15	TC	Smirnov et al. (2003)
Matachewan dikes (Canada)	MH	2460 ± 14	2.53 ± 0.93	12/12	MW	Halls et al. (2004)
	MM		2.80 ± 0.87	5/26	TC	Macouin et al. (2003)
Dolerite dike (West Greenland)	WG1	2585 ± 21	2.30 ± 0.42	1/14	TC	Miki et al. (2009)
Dolerite dikes (Slave Province, Canada)	SP1	2631 ± 11	9.0 ± 0.2	1/7	TC	Yoshihara and Hamano (2000)
	SP2		6.3 ± 0.2	1/5	TC	
Stillwater complex (Montana, USA)	SC	2701 ± 8	5.05 ± 1.46*	53/114	TC	Selkin et al. (2008)
Pilbara lava flow (Western Australia)	PL	2721 ± 4	4.7 ± 0.6**	1/3	TC	Biggin et al. (2009)
Dolerite dike (West Greenland)	WG2	2752 ± 63	1.9 ± 0.6	1/12	TC	Morimoto et al. (1997)
Modipe Gabbro (Botswana)	MG	2784 ± 4	6.4 ± 0.4***	1/18	TC	Muxworthy et al. (2013)

Notes: * Corrected for the cooling rate, anisotropy of remanent magnetization, and non-linear TRM acquisition; ** corrected for magnetomineralogical alteration during laboratory experiments; *** corrected for the cooling rate.

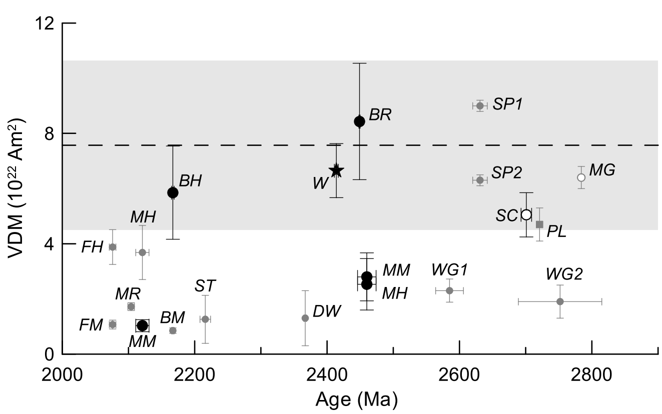

Fig. 7. Neoarchean and early Paleoproterozoic virtual dipole moment (VDM) data (with 1σ uncertainties) (Table 2). Larger black (smaller grey) symbols show the VDM means based on four or more (three or less) sites. Closed and open symbols show the results from quickly (extrusives, shallow intrusions) and slowly cooled rocks, respectively.

yses on single plagioclase crystals from four dikes resulted in the mean value of 8.43 ± 2.11 × 10^{22} A m^2 (Smirnov et al., 2003). The slightly older, ~2.46 Ga Matachewan mafic dikes (Ontario, Canada) yielded substantially lower paleointensity values. Macouin et al. (2003) reported a mean VDM value of 2.80±0.87×10^{22} A m^2 from five dikes, while Halls et al. (2004) used the microwave-Thellier technique (e.g., Walton, 1991; Walton et al., 1996) to obtain a mean VDM value of 2.53 ± 0.93 × 10^{22} A m^2 from twelve Matachewan dikes. McArdle et al. (2004) and Smirnov and Tarduno (2005) reported similar low VDM values obtained with the Thellier method from four and two Matachewan dikes, respectively.

For the Neoarchean era, Miki et al. (2009) reported a low VDM value of 2.30 ± 0.42 × 10^{22} A m^2 from a single ~ 2.59 Ga dolerite dike from West Greenland. A similar VDM of 1.9 ± 0.6 × 10^{22} A m^2 was reported from a nearby ~ 2.75 Ga dolerite dike (Morimoto et al., 1997). On the other hand, Yoshihara and Hamano (2000) reported relatively high mean paleointensity values of 6.3 ± 0.2 × 10^{22} A m^2 and 9.0 ± 0.2 × 10^{22} A m^2 from two ~ 2.63 Ga dolerite dikes from the Slave Province (Canada). Finally, Biggin et al. (2009) reported a 4.7 ± 0.6 × 10^{22} A m^2 VDM value from a single ~2.72 Ma lava flow from the East Pilbara craton (Western Australia).

The Neoarchean data also include two Thellier paleointensity determinations based on slowly cooled rocks. Selkin et al. (2008) obtained a mean VDM of 5.05 ± 1.46 × 10^{22} A m^2 from 53 sites of the ~ 2.7 Ga Stillwater Complex (Montana, USA) after correcting their data for the cooling rate, remanence anisotropy, and non-linear TRM acquisition. Muxworthy et al. (2013) reported a mean cooling-rate-corrected VDM of 6.4 ± 0.4 × 10^{22} A m^2 from a single site from the ~2.78 Ga Modipe Gabbro (Botswana), although as noted by Tarduno et al. (2014), this result did not include any estimates of post-emplacement tilting, which, due to the steepness of the in-situ remanence vector, would likely cause underestimation of the true field strength.

The early Paleoproterozoic data are based on paleointensity investigations of several mafic dike swarms. Valet et al. (2014) obtained a low paleointensity value of 1.30 ± 1.00 × 10^{22} A m^2 from two ~2.37 Ga dikes from the Dharwar dike swarm in southern India. Macouin et al. (2003) reported similar low paleointensity values obtained with the Thellier method from ~2.22 Ga Senneterre dikes (the mean VDM = 1.26 ± 0.87 × 10^{22} A m^2), the ~2.17 Ga Biscotasing dikes (0.85±0.10×10^{22} A m^2), the ~2.12 Ga Marathon dikes ($1.03 \pm 0.22 \times 10^{22}$ A m^2), and the ~2.076 Ga Fort Frances dikes ($1.07 \pm 0.16 \times 10^{22}$ A m^2). Investigation of several of these dike swarms using the microwave method (Halls et al., 2004), however, resulted in systematically higher paleointensity values: $5.85 \pm 1.69 \times 10^{22}$ A m^2 for the Biscotasing dikes, $3.88 \pm 0.63 \times 10^{22}$ A m^2 for the Fort Frances dikes, and $3.68 \pm 0.98 \times 10^{22}$ A m^2 and $1.72 \pm 0.14 \times 10^{22}$ A m^2 for the normal and reversed polarity Marathon dikes, respectively. Halls et al. (2004) suggested that the difference between their results and those of Macouin et al. (2003) may be due to the presence of secondary magnetizations in the samples used in the earlier study.

Overall, the early-Paleoproterozoic–Neoarchean data do not reveal any obvious long-term trends in the field strength behavior (Fig. 7, Table 2). However, the data show a significant scatter with the abundance of low paleointensity values. While some of these weak-field values may represent the secular variation of geomagnetic field, some may reflect the effect of TCRM (Smirnov and Tarduno, 2005). We note that the formation and relative strength of TCRM ultimately depend on the cessation temperature and the resulting oxide assemblage of originating sub-solidus reactions, which in turn are controlled by the oxygen fugacity, temperature, cooling rate, and initial magma composition (e.g., Buddington and Lindsley, 1964; Frost and Lindsley, 1991).

5.3. Implications for the early Paleoproterozoic-Neoarchean geodynamo

The mean and range of paleofield values obtained from the Widgiemooltha dikes are within the range of paleointensity values observed for the last 10 million years (e.g., Tarduno and Smirnov, 2004) (Fig. 7). Prior paleointensity and paleodirectional studies (e.g., Smirnov et al., 2003; Smirnov and Tarduno, 2004; Coe and Glatzmaier, 2006; Tarduno et al., 2007, 2010; Biggin et al., 2009; Smirnov et al., 2011; Muxworthy et al., 2013) also point to existence and sustenance of a dipolar, stable, and relatively strong magnetic field through the Archean–Proterozoic transition. A purely thermally-driven geodynamo is generally considered incapable of sustaining such a field (e.g., Gubbins et al., 2003; Costin and Butler, 2006; Hori et al., 2014) although alternative views have been presented (Aubert et al., 2009). Compositional convection in the outer core, arising from inner core growth, appears necessary to drive an enduring dipolar geodynamo with the stable and strong characteristics implied by the Neoarchean–Paleoproterozoic data. In particular, based on the analyses of paleosecular variation in the Proterozoic and Neoarchean, Smirnov et al. (2011) suggested an early onset of inner core growth possibly linked to cooling of the lower mantle by deep subduction between ~3.5 and 2.0 Ga.

The relatively old inner core age implied by the paleointensity and paleodirectional data for the Proterozoic and Neoarchean favors the presence of radiogenic elements in the core (Buffett, 2002). However, an old inner core is inconsistent with the recent models of Earth's thermal evolution that suggest a much younger inner core nucleation age (e.g., Aubert et al., 2009). Furthermore, the existence of a strong dipolar field since the Neoarchean is difficult to reconcile with the recent estimates of thermal conductivity of liquid iron under the conditions in Earth's core that make it even more difficult to maintain a geodynamo throughout geological history (Pozzo et al., 2012; de Koker et al., 2012; Buffett, 2012). Resolution of these important questions may require a substantial modification of our current paradigm about geodynamo generation, perhaps even involving consideration of an additional, now unknown energy source (Buffett, 2012). For example, Ziegler and Stegman (2013) suggested that a strong and more antisymmetric field could have been generated within a basal-mantle magma ocean before ~2.45 Ga. The current challenges experienced by the Earth's thermal history and geodynamo models emphasize the importance of observational paleointensity and paleomagnetic data, such as presented herein, that provide important constraints for the development of more realistic, Earth-like models of long-term geodynamo evolution.

6. Conclusions

High-quality, absolute paleointensity determinations obtained from the ~2.41 Ga Widgiemooltha dikes demonstrate that the LTD-Thellier approach represents a viable method to derive reliable estimates of the Earth's paleofield strength from the Precambrian rocks that are not suitable for conventional Thellier analyses. The relatively strong paleointensity values obtained from the Widgiemooltha dikes, similar to those of the more recent field, provide an additional support to the existence of a compositional convection-driven geodynamo established as early as the Archean-Proterozoic boundary. Acquisition of additional paleointensity data using the LTD-Thellier method, and other novel approaches such as paleointensity determinations from single silicate crystals (e.g., Tarduno et al., 2006), are crucial for constraining and improving the models of Earth's thermal history and geodynamo.

Acknowledgements

We thank Danford Moore, Ian Rose, and Taylor Kilian for help in the field and with the laboratory measurements, Klaydson Celino, Lauren Greenwood and Elissa Barris for help with paleointensity measurements, and Evgeniy Kulakov for help with SEM analyses. We thank the Geological Survey of Western Australia, the University of Western Australia, Michael Wingate, Martin Van Kranendonk and Peter Cawood for logistical support. Comments by Roman Leonhardt and an anonymous reviewer greatly improved our manuscript. This research was supported by the U.S. National Science Foundation (EAR-0711453) and the David and Lucile Packard Foundation.

References

Arai, Y., 1963. Secular variation in the intensity of the past geomagnetic field. M.S. thesis. Univ. of Tokyo, Tokyo, Japan. 84 pp.
Aubert, J., Labrosse, S., Poitou, C., 2009. Modelling the paleo-evolution of the geodynamo. Geophys. J. Int. 179, 1414–1428.
Aubert, J., Tarduno, J.A., Johnson, C.L., 2010. Observations and models of the long-term evolution of Earth's magnetic field. Space Sci. Rev. 155, 337–370.
Biggin, A.J., Strik, G.H.M.A., Langereis, C.G., 2009. The intensity of the geomagnetic field in the late-Archaean: new measurements and an analysis of the updated IAGA palaeointensity database. Earth Planets Space 61, 9–22.
Bolshakov, A.S., Shcherbakova, V.V., 1979. A thermomagnetic criterion for determining the domain structure of ferrimagnetics (translated from Russian). Izv. Phys. Solid Earth 15, 111–117.
Buddington, A.F., Lindsley, D.H., 1964. Iron–titanium oxide minerals and synthetic equivalents. J. Petrol. 5, 310–357.
Buffett, B.A., 2002. Estimates of heat flow in the deep mantle based on the power requirements for the geodynamo. Geophys. Res. Lett. 29, 1566. http://dx.doi.org/10.1029/2001GL014649.
Buffett, B., 2012. Geomagnetism under scrutiny. Nature 485, 319–320.
Celino, K.R., Trindade, R.I.F., Tohver, E., 2007. LTD-Thellier paleointensity of 1.2 Ga Nova Floresta mafic rocks (Amazon craton). Geophys. Res. Lett. 34, L12306. http://dx.doi.org/10.1029/2007GL029550.
Clark, D.A., Schmidt, P.W., 1982. Theoretical analysis of thermomagnetic properties, low-temperature hysteresis and domain structure of titanomagnetites. Phys. Earth Planet. Inter. 30, 300–316.
Coe, R.S., 1967. The determination of paleointensities of the Earth's magnetic field with emphasis on mechanisms which could cause non-ideal behaviour in Thelliers method. J. Geomagn. Geoelectr. 19, 157–179.
Coe, R.S., Grommé, S., Mankinen, E.A., 1978. Geomagnetic paleointensities from radiocarbon dated lava flows on Hawaii and the question of the Pacific nondipole low. J. Geophys. Res. 83, 1740–1756.
Coe, R.S., Glatzmaier, G.A., 2006. Symmetry and stability of the geomagnetic field. Geophys. Res. Lett. 33, L21311. http://dx.doi.org/10.1029/2006GL027903.
Costin, S.O., Butler, S.L., 2006. Modelling the effects of internal heating in the core and lowermost mantle on the earth's magnetic history. Phys. Earth Planet. Inter. 157, 55–71.

Day, R., Fuller, M., Schmidt, V.A., 1977. Hysteresis properties of titanomagnetites: grain-size and compositional dependence. Phys. Earth Planet. Inter. 13, 260–267.

Dodson, M.H., McClelland-Brown, E., 1980. Magnetic blocking temperatures of single-domain grains during slow cooling. J. Geophys. Res. 85, 2625–2637.

Doehler, J.S., Heaman, L.M., 1998. 2.41 Ga U–Pb baddeleyite ages for two gabbroic dykes from the Widgiemooltha swarm, Western Australia: a Yilgarn–Lewisian connection? In: GSA Annual Meeting, Toronto Ontario, p. A-291.

Dunlop, D.J., 1974. Thermal enhancement of magnetic susceptibility. J. Geophys. 40, 439–451.

Dunlop, D.J., Özdemir, Ö., 1997. Rock Magnetism: Fundamentals and Frontiers. Cambridge University Press, Cambridge. 573 pp.

Dunlop, D.J., 2002. Theory and application of the Day plot (M_{rs}/M_s versus H_{cr}/H_c): 1. Theoretical curves and tests using titanomagnetite data. J. Geophys. Res. 107. http://dx.doi.org/10.1029/2001JB000486. 2056.

Engelmann, R., Kontny, A., Lattard, D., 2010. Low-temperature magnetism of synthetic Fe–Ti oxide assemblages. J. Geophys. Res. 115, B12107. http://dx.doi.org/10.1029/2010JB000865.

Ernst, R.E., Buchan, K.L., 1997. Giant radiating dyke swarms: their use in identifying pre-Mesozoic large igneous provinces and mantle plumes. In: Mahoney, J., Coffin, M. (Eds.), Large Igneous Provinces: Continental, Oceanic, and Planetary Volcanism. In: AGU Geophysical Monograph Series, vol. 100, pp. 297–333.

Evans, M.E., 1968. Magnetization of dikes: a study of the paleomagnetism of the Widgiemooltha dike suite, Western Australia. J. Geophys. Res. 73, 3261–3270.

Evans, D.A.D., 2006. Proterozoic low orbital obliquity and axial-dipolar geomagnetic field from evaporite palaeolatitudes. Nature 444, 51–55.

Fabian, K., 2009. Thermochemical remanence acquisition in single-domain particle ensembles: a case for possible overestimation of the geomagnetic paleointensity. Geochem. Geophys. Geosyst. 10, Q06Z03. http://dx.doi.org/10.1029/2009GC002420.

Ferk, A., Leonhardt, R., Hess, K.U., Koch, S., Egli, R., Krasa, D., Dingwell, D.B., 2014. Influence of cooling rate on thermoremanence of magnetite grains: identifying the role of different magnetic domain states. J. Geophys. Res. 119, 1599–1606.

Fletcher, I.A., Libby, W.G., Rosman, K.J.R., 1987. Sm–Nd dating of the 2411 Ma Jimberlana dyke, Yilgarn block, Western Australia. Aust. J. Earth Sci. 34, 523–525.

French, J.E., Heaman, L.M., Chacko, T., 2002. Feasibility of chemical U–Th-total Pb baddeleyite dating by electron microprobe. Chem. Geol. 188, 85–104.

Frost, B.R., Lindsley, D.H., 1991. Occurrence of iron–titanium oxides in igneous rocks. Rev. Miner. 25, 434–468.

Gubbins, D., Alfe, D., Masters, G., Price, D.G., Gillan, M.J., 2003. Can the Earth's dynamo run on heat alone? Geophys. J. Int. 155, 609–622.

Halgedahl, S.E., Day, R., Fuller, M., 1980. The effect of cooling rate on the intensity of weak field TRM in single-domain magnetite. J. Geophys. Res. 85, 3690–3698.

Hallberg, J.A., 1987. Postcratonization mafic and ultramafic dykes of the Yilgarn Block. Aust. J. Earth Sci. 34, 135–149.

Halls, H.C., McArdle, N.J., Gratton, M.N., Hill, M.J., Shaw, J., 2004. Microwave paleointensities from dyke chilled margins: a way to obtain long term variations in geodynamo intensity for the last three billion years. Phys. Earth Planet. Inter. 147, 183–195.

Halls, H.C., 2008. The importance of integrating paleomagnetic studies of Proterozoic dykes with U–Pb geochronology and geochemistry. In: Srivastava, R.K., Sivaji, C., Chalapathi Rao, N.V. (Eds.), Indian Dykes: Geochemistry, Geophysics and Geochronology. Narosa Publishing House Pvt Ltd., New Delhi, India, pp. 1–22.

Hirt, A.M., Gehring, A.U., 1991. Thermal alteration of the magnetic mineralogy in ferruginous rocks. J. Geophys. Res. 96, 9947–9953.

Hori, K., Wicht, J., Dietrich, W., 2014. Ancient dynamos of terrestrial planets more sensitive to core–mantle boundary heat flows. Planet. Space Sci. 98, 30–40.

Jaeger, J.C., 1968. Cooling and solidification of igneous rocks. In: Hess, H.H., Poldervaart, A. (Eds.), Basalts: The Poldervaart Treatise on Rocks of Basaltic Composition. Interscience Publishers, New York, London, Sydney, pp. 503–536.

Kakol, Z., Sabol, J., Honig, J.M., 1991. Magnetic anisotropy of titanomagnetites $Fe_{3-x}Ti_xO_4$, $0 \le x \le 0.55$. Phys. Rev. B, Condens. Matter Mater. Phys. 44, 2198–2204.

Kakol, Z., Sabol, J., Stickler, J., Honig, J.M., 1992. Effect of low-level titanium (IV) doping on the resistivity of magnetite near the Verwey transition. Phys. Rev. B, Condens. Matter Mater. Phys. 46, 1975–1978.

Kobayashi, K., Fuller, M., 1968. Stable remanence and memory phenomenon in multidomain materials with special reference to magnetite. Philos. Mag. 18, 601–611.

de Koker, N., Steinle-Neumann, G., Vlček, V., 2012. Electrical resistivity and thermal conductivity of liquid Fe alloys at high P and T, and heat flux in Earth's core. Proc. Natl. Acad. Sci. USA 109, 4070–4073.

Kosterov, A.A., Prévot, M., 1998. Possible mechanisms causing failure of Thellier palaeointensity experiments in some basalts. Geophys. J. Int. 134, 554–572.

Kosterov, A., Conte, G., Goguitchaichvili, A., Urrutia-Fucugauchi, J., 2009. Low-temperature magnetic properties of andesitic rocks from Popocatepetl stratovolcano, Mexico. Earth Planets Space 61, 133–142.

Kulakov, E.V., Smirnov, A.V., Diehl, J.F., 2013. Absolute geomagnetic paleointensity as recorded by ~1.09 Ga Lake Shore Traps (Keweenaw Peninsula, Michigan). Stud. Geophys. Geod. 57, 565–584.

Leonhardt, R., Hufenbecher, F., Heider, F., Soffel, H.C., 2000. High absolute paleointensity during a mid Miocene excursion of the Earth's magnetic field. Earth Planet. Sci. Lett. 184, 141–154.

Leonhardt, R., Heunemann, C., Krása, D., 2004. Analyzing absolute paleointensity determinations: acceptance criteria and the software ThellierTool4.0. Geochem. Geophys. Geosyst. 5, Q12016. http://dx.doi.org/10.1029/2004GC000807.

Levi, S., Merrill, R.T., 1978. Properties of single-domain, pseudo-singledomain, and multidomain magnetite. J. Geophys. Res. 83, 309–323.

Macouin, M., Valet, J.P., Besse, J., Buchan, K., Ernst, R., LeGoff, M., Scharer, U., 2003. Low paleointensities recorded in 1 to 2.4 Ga Proterozoic dykes, Superior Province, Canada. Earth Planet. Sci. Lett. 213, 79–95. http://dx.doi.org/10.1016/S0012-821X(03)00243-7.

Macouin, M., Valet, J.P., Besse, J., Buchan, K., Ernst, R., 2006. Absolute paleointensity at 1.27 Ga from the Mackenzie dyke swarm (Canada). Geochem. Geophys. Geosyst. 7, Q01H21. http://dx.doi.org/10.1029/2005GC000960.

McArdle, N.J., Halls, H.C., Shaw, J., 2004. Rock magnetic studies and a comparison between microwave and Thellier palaeointensities for Canadian Precambrian dykes. Phys. Earth Planet. Inter. 147, 247–254.

McClay, K.R., 1974. Single-domain magnetite in the Jimberlana norite, Western Australia. Earth Planet. Sci. Lett. 21, 367–376.

McClelland-Brown, E., 1984. Experiments on TRM intensity dependence on cooling rate. Geophys. Res. Lett. 11, 205–208.

Miki, M., Taniguchi, A., Yokoyama, M., Gouzu, C., Hyodo, H., Uno, K., Zaman, H., Otofuji, Y., 2009. Palaeomagnetism and geochronology of the Proterozoic dolerite dyke from southwest Greenland: indication of low palaeointensity. Geophys. J. Int. 179, 18–34.

Morimoto, C., Otofuji, Y., Miki, M., Tanaka, H., Itaya, T., 1997. Preliminary paleomagnetic results of an Archean dolerite dike of West Greenland geomagnetic field intensity at 2.8 Ga. Geophys. J. Int. 128, 585–593.

Muxworthy, A.R., Evans, M.E., Scourfield, S.J., King, J.G., 2013. Paleointensity results from the late-Archaean Modipe Gabbro of Botswana. Geochem. Geophys. Geosyst. 14, 2198–2205.

Nagata, T., Arai, Y., Momose, K., 1963. Secular variation of the geomagnetic total force during the last 5000 years. J. Geophys. Res. 207, 173–184.

Nagata, T., Kobayashi, K., 1963. Thermo-chemical remanent magnetization of rocks. Nature 197, 476–477.

Nemchin, A.A., Pidgeon, R.T., 1998. Precise conventional and SHRIMP baddeleyite U–Pb age for the Binneringie Dyke, near Narrogin, Western Australia. Aust. J. Earth Sci. 45, 673–675.

Ozima, M., Ozima, M., Akimoto, S., 1964. Low temperature characteristics of remanent magnetization of magnetite: self-reversal and recovery phenomena of remanent magnetization. J. Geomagn. Geoelectr. 16, 165–177.

Ozima, M., Yin, Q.Z., Podosek, F.A., Miura, Y.N., 2008. Toward understanding early Earth evolution: prescription for approach from terrestrial noble gas and light element records in lunar soils. Proc. Natl. Acad. Sci. USA 105, 17654–17658.

Parker, A.J., Rickwood, P.C., Baillie, P.W., McClenaghan, M.P., Boyd, D.M., Freeman, M.J., Pietsch, B.A., Murray, C.G., Myers, J.S., 1987. Mafic dyke swarms of Australia. In: Halls, H.C., Fahrig, W.F. (Eds.), Mafic Dyke Swarms Geological, vol. 34. Association of Canada Special Paper. St. John's, Newfoundland, pp. 401–417.

Pozzo, M., Davies, C., Gubbins, D., Alfê, D., 2012. Thermal and electrical conductivity of iron at Earth's core conditions. Nature 485, 355–358.

Schmidt, P.W., 1993. Paleomagnetic cleaning strategies. Phys. Earth Planet. Inter. 76, 169–178.

Selkin, P.A., Gee, J.S., Meurer, W.P., Hemming, S.R., 2008. Paleointensity record from the 2.7 Ga Stillwater Complex, Montana. Geochem. Geophys. Geosyst. 9, Q12023. http://dx.doi.org/10.1029/2008GC001950.

Shashkanov, V.A., Metallova, V.V., 1972. Violation of Thellier's law for partial thermoremanent magnetization. Izv. Acad. Sci. U.S.S.R., Phys. Solid Earth 8, 180–184 (English translation).

Shcherbakov, V.P., Shcherbakova, V.V., 2001. On the suitability of the Thellier method of palaeointensity determination on pseudo-single-domain and multidomain grains. Geophys. J. Int. 146, 20–30.

Shcherbakova, V.V., Lubnina, N.V., Shcherbakov, V.P., Mertanen, S., Zhidkov, G.V., Vasilieva, T.I., Tsel'movich, V.A., 2008. Paleointensity and paleodirectional studies of early Riphaean dyke complexes in the Lake Ladoga region (Northwestern Russia). Geophys. J. Int. 175, 433–448.

Sinnhuber, M., Burrows, J.P., Chipperfield, M.P., Jackman, C.H., Kallenrode, M.B., Kunzi, K.F., Quack, M., 2003. A model study of the impact of magnetic field structure on atmospheric composition during solar proton events. Geophys. Res. Lett. 30, 1818, 2003.

Smirnov, A.V., Tarduno, J.A., Pisakin, B.N., 2003. Paleointensity of the early geodynamo (2.45 Ga) as recorded in Karelia: a single crystal approach. Geology 31, 415–418.

Smirnov, A.V., Tarduno, J.A., 2004. Secular variation of the Late Archean–Early Proterozoic geodynamo. Geophys. Res. Lett. 31, L16607. http://dx.doi.org/10.1029/2004GL020333.

Smirnov, A.V., Bauch, D.G., Tarduno, J.A., 2005. Temperature dependence of magnetic susceptibility as a potential indicator of fine-scale oxyexsolution in igneous rocks. In: Fall Meet. Suppl. Eos Trans. AGU 86 (52). Abstract GP13A-0040.

Smirnov, A.V., Tarduno, J.A., 2005. Thermochemical remanent magnetization in Precambrian rocks: are we sure the geomagnetic field was weak? J. Geophys. Res. 110, B06103. http://dx.doi.org/10.1029/2004JB003445.
Smirnov, A.V., Tarduno, J.A., Evans, D.A.D., 2011. Evolving core conditions ca. 2 billion years ago detected by paleosecular variation. Phys. Earth Planet. Inter. 187, 225–231.
Smirnov, A.V., Evans, D.A.D., Ernst, R.E., Soderlund, U., Li, Z.-X., 2013. Trading partners: tectonic ancestry of southern Africa and western Australia, in Archean supercratons Vaalbara and Zimgarn. Precambrian Res. 224, 11–22.
Sofoulis, J., 1966. Widgiemooltha, Western Australia. Geological Survey of Western Australia, 1:250 000 Geology series explanatory notes, Sheet SH/51-14.
Stevenson, D.J., Spohn, T., Schubert, G., 1983. Magnetism and thermal evolution of the terrestrial planets. Icarus 54, 466–489.
Syono, Y., 1965. Magnetocrystalline anisotropy and magnetostriction of Fe_3O_4–Fe_2TiO_4 series, with special application to rock magnetism. Jpn. J. Geophys. 4, 71–143.
Tarduno, J.A., Smirnov, A.V., 2004. The paradox of low field values and the long-term history of the geodynamo. In: Channell, J.E.T., Kent, D.V., Lowrie, W., Meert, J.G. (Eds.), Timescale of the Paleomagnetic Field. In: AGU Geophysical Monograph, vol. 145, pp. 75–84.
Tarduno, J.A., Cottrell, R.D., Smirnov, A.V., 2006. The paleomagnetism of single silicate crystals: recording geomagnetic field strength during mixed polarity intervals, superchrons, and inner core growth. Rev. Geophys. 44, RG1002. http://dx.doi.org/10.1029/2005RG000189.
Tarduno, J.A., Cottrell, R.D., Watkeys, M.K., Bauch, D., 2007. Geomagnetic field strength 3.2 billion years ago recorded by single silicate crystals. Nature 446, 657–660.
Tarduno, J.A., Cottrell, R.D., Watkeys, M.K., Hofmann, A., Doubrovine, P.V., Mamajek, E., Liu, D., Sibeck, D.G., Neukirch, L.P., Usui, Y., 2010. Geodynamo, solar wind and magnetopause 3.45 billion years ago. Science 327, 1238–1240.
Tarduno, J.A., Blackman, E.G., Mamajek, E.E., 2014. Detecting the oldest geodynamo and attendant shielding from the solar wind: implications for habitability. Phys. Earth Planet. Inter. 233, 68–87.
Tauxe, L., Yamazaki, T., 2007. Paleointensities. In: Schubert, G. (Ed.), Treatise on Geophysics. In: Geomagnetism, vol. 5. Elsevier Ltd., Oxford, pp. 509–564.
Thellier, E., 1941. Sur la vérification d'une méthode permettant de déterminer l'intensité du champ magnétique terrestre dans la Passé. C. R. Acad. Sci. 212, 281–283.
Thellier, E., Thellier, O., 1959. Sur l'intensité du champ magnétique terrestre dans le passé historique et géologique. Ann. Geophys. 15, 285–376.
Valet, J.-P., Besse, J., Kumar, A., Vadakke-Chanat, S., Philippe, E., 2014. The intensity of the geomagnetic field from 2.4 Ga old Indian dykes. Geochem. Geophys. Geosyst. 15, 2426–2437. http://dx.doi.org/10.1002/2014GC005296.
Van der Voo, R., 1990. The reliability of paleomagnetic data. Tectonophysics 184, 1–9.
Verwey, E.J.W., 1939. Electronic conduction of magnetite (Fe_3O_4) and its transition point at low-temperature. Nature 44, 327–328.
Walton, D., 1991. A new technique for determining palaeomagnetic intensities. J. Geomagn. Geoelectr. 43, 333–339.
Walton, D., Snape, S., Rolph, T.C., Shaw, J., Share, J., 1996. Application of ferrimagnetic resonance heating to palaeointensity determinations. Phys. Earth Planet. Inter. 94, 183–186.
Winklhofer, M., Fabian, K., Heider, F., 1997. Magnetic blocking temperatures of magnetite calculated with a three-dimensional micromagnetic model. J. Geophys. Res. 102, 22695–22709.
Xu, S., Dunlop, D.J., 2004. Thellier paleointensity theory and experiments for multidomain grains. J. Geophys. Res. 109, B07103. http://dx.doi.org/10.1029/2004JB003024.
Yoshihara, A., Hamano, Y., 2000. Intensity of the Earth's magnetic field in late Archean obtained from diabase dikes of the Slave Province, Canada. Phys. Earth Planet. Inter. 117, 295–307.
Yoshihara, A., Hamano, Y., 2004. Paleomagnetic constraints on the Archean geomagnetic field intensity obtained from komatiites of the Barberton and Belingwe greenstone belts, South Africa and Zimbabwe. Precambrian Res. 131, 111–142.
Yu, Y., 2011. Importance of cooling rate dependence of thermoremanence in paleointensity determination. J. Geophys. Res. 116, B09101. http://dx.doi.org/10.1029/2011JB008388.
Ziegler, L.B., Stegman, D.R., 2013. Implications of a long-lived basal magma ocean in generating Earth's ancient magnetic field. Geochem. Geophys. Geosyst. 14, 4735–4742. http://dx.doi.org/10.1002/2013GC005001.